

Search for Heavy Charged Particles and for Particles with Anomalous Charge in e^+e^- Collisions at LEP

The OPAL Collaboration

Abstract

Using the OPAL data accumulated in 1991–1993 amounting to 74 pb^{-1} of integrated luminosity, corresponding to 1.64×10^6 selected multi-hadronic events, a search has been performed for charged particles with unusual mass or unusual charge. The mass was determined from a combination of momentum and ionization energy loss measurements. No isolation criteria were applied to the tracks examined, so that both isolated particles and particles produced in jets were valid candidates. For particles with charge $Q/e = -1$, one candidate with a mass of approximately $4.2 \text{ GeV}/c^2$ was found, which is compatible with the background rate expected according to a Monte Carlo simulation. The implications of this search for the mass limits of a conjectured stable or quasi-stable charged gluino composite $(\tilde{g}q\bar{q}')^\pm$ are discussed. Limits are also presented for the production of fractionally-charged particles with $Q/e = \pm 2/3$ and $\pm 4/3$ as well as for particles with $Q/e = \pm 2$.

(to be submitted to Zeit. Phys. C)

The OPAL Collaboration

R. Akers¹⁶, G. Alexander²³, J. Allison¹⁶, K. Ametewee²⁵, K.J. Anderson⁹, S. Arcelli², S. Asai²⁴, D. Axen²⁹,
 G. Azuelos^{18,a}, A.H. Ball¹⁷, E. Barberio²⁶, R.J. Barlow¹⁶, R. Bartoldus³, J.R. Batley⁵, G. Beaudoin¹⁸,
 A. Beck²³, G.A. Beck¹³, C. Beeston¹⁶, T. Behnke²⁷, K.W. Bell²⁰, G. Bella²³, S. Bentvelsen⁸, P. Berlich¹⁰,
 S. Bethke³², O. Biebel³², I.J. Bloodworth¹, P. Bock¹¹, H.M. Bosch¹¹, M. Boutemour¹⁸, S. Braibant¹²,
 P. Bright-Thomas²⁵, R.M. Brown²⁰, A. Buijs⁸, H.J. Burckhart⁸, R. Bürgin¹⁰, C. Burgard²⁷, N. Capdevielle¹⁸,
 P. Capiluppi², R.K. Carnegie⁶, A.A. Carter¹³, J.R. Carter⁵, C.Y. Chang¹⁷, C. Charlesworth⁶, D.G. Charlton^{1,b},
 S.L. Chu⁴, P.E.L. Clarke¹⁵, J.C. Clayton¹, S.G. Clowes¹⁶, I. Cohen²³, J.E. Conboy¹⁵, O.C. Cooke¹⁶,
 M. Cuffiani², S. Dado²², C. Dallapiccola¹⁷, G.M. Dallavalle², C. Darling³¹, S. De Jong¹², L.A. del Pozo⁸,
 H. Deng¹⁷, M. Dittmar⁴, M.S. Dixit⁷, E. do Couto e Silva¹², J.E. Duboscq⁸, E. Duchovni²⁶, G. Duckeck⁸,
 I.P. Duerdoth¹⁶, U.C. Dunwoody⁵, J.E.G. Edwards¹⁶, P.A. Elcombe⁵, P.G. Estabrooks⁶, E. Etzion²³,
 H.G. Evans⁹, F. Fabbri², B. Fabbro²¹, M. Fanti², P. Fath¹¹, M. Fierro², M. Fincke-Keeler²⁸, H.M. Fischer³,
 P. Fischer³, R. Folman²⁶, D.G. Fong¹⁷, M. Foucher¹⁷, H. Fukui²⁴, A. Fürtjes⁸, P. Gagnon⁶, A. Gaidot²¹,
 J.W. Gary⁴, J. Gascon¹⁸, N.I. Geddes²⁰, C. Geich-Gimbel³, S.W. Gensler⁹, F.X. Gentit²¹, T. Geralis²⁰,
 G. Giacomelli², P. Giacomelli⁴, R. Giacomelli², V. Gibson⁵, W.R. Gibson¹³, J.D. Gillies²⁰, J. Goldberg²²,
 D.M. Gingrich^{30,a}, M.J. Goodrick⁵, W. Gorn⁴, C. Grandi², E. Gross²⁶, J. Hagemann²⁷, G.G. Hanson¹²,
 M. Hansroul⁸, C.K. Hargrove⁷, P.A. Hart⁹, M. Hauschild⁸, C.M. Hawkes⁸, E. Heflin⁴, R.J. Hemingway⁶,
 G. Herten¹⁰, R.D. Heuer⁸, J.C. Hill⁵, S.J. Hillier⁸, T. Hilse¹⁰, P.R. Hobson²⁵, D. Hochman²⁶, R.J. Homer¹,
 A.K. Honma^{28,a}, R. Howard²⁹, R.E. Hughes-Jones¹⁶, P. Igo-Kemenes¹¹, D.C. Imrie²⁵, A. Jawahery¹⁷,
 P.W. Jeffreys²⁰, H. Jeremie¹⁸, M. Jimack¹, M. Jones⁶, R.W.L. Jones⁸, P. Jovanovic¹, C. Jui⁴, D. Karlen⁶,
 J. Kanzaki²⁴, K. Kawagoe²⁴, T. Kawamoto²⁴, R.K. Keeler²⁸, R.G. Kellogg¹⁷, B.W. Kennedy²⁰, B. King⁸,
 J. King¹³, J. Kirk²⁹, S. Kluth⁵, T. Kobayashi²⁴, M. Kobel¹⁰, D.S. Koetke⁶, T.P. Kokott³, S. Komamiya²⁴,
 R. Kowalewski⁸, T. Kress¹¹, P. Krieger⁶, J. von Krogh¹¹, P. Kyberd¹³, G.D. Lafferty¹⁶, H. Lafoux⁸,
 R. Lahmann¹⁷, W.P. Lai¹⁹, J. Lauber⁸, J.G. Layter⁴, P. Leblanc¹⁸, A.M. Lee³¹, E. Lefebvre¹⁸, D. Lellouch²⁶,
 C. Leroy¹⁸, J. Letts², L. Levinson²⁶, S.L. Lloyd¹³, F.K. Loebinger¹⁶, G.D. Long¹⁷, B. Lorazo¹⁸, M.J. Losty⁷,
 X.C. Lou⁸, J. Ludwig¹⁰, A. Luig¹⁰, M. Mannelli⁸, S. Marcellini², C. Markus³, A.J. Martin¹³, J.P. Martin¹⁸,
 T. Mashimo²⁴, W. Matthews²⁵, P. Mättig³, U. Maur³, J. McKenna²⁹, T.J. McMahon¹, A.I. McNab¹³,
 F. Meijers⁸, F.S. Merritt⁹, H. Mes⁷, A. Michelini⁸, R.P. Middleton²⁰, G. Mikenberg²⁶, D.J. Miller¹⁵, R. Mir²⁶,
 W. Mohr¹⁰, A. Montanari², T. Mori²⁴, M. Morii²⁴, U. Müller³, B. Nellen³, B. Nijhar¹⁶, S.W. O’Neale¹,
 F.G. Oakham⁷, F. Odorici², H.O. Ogren¹², N.J. Oldershaw¹⁶, C.J. Oram^{28,a}, M.J. Oreglia⁹, S. Orito²⁴,
 F. Palmonari², J.P. Pansart²¹, G.N. Patrick²⁰, M.J. Pearce¹, P.D. Phillips¹⁶, J.E. Pilcher⁹, J. Pinfold³⁰,
 D.E. Plane⁸, P. Poffenberger²⁸, B. Poli², A. Posthaus³, T.W. Pritchard¹³, H. Przysieznik³⁰, M.W. Redmond⁸,
 D.L. Rees⁸, D. Rigby¹, M.G. Rison⁵, S.A. Robins¹³, D. Robinson⁵, N. Rodning³⁰, J.M. Roney²⁸, E. Ros⁸,
 A.M. Rossi², M. Rosvick²⁸, P. Routenburg³⁰, Y. Rozen⁸, K. Runge¹⁰, O. Runolfsson⁸, D.R. Rust¹², M. Sasaki²⁴,
 C. Sbarra², A.D. Schaile⁸, O. Schaile¹⁰, F. Scharf³, P. Scharff-Hansen⁸, P. Schenk⁴, B. Schmitt³, M. Schröder⁸,
 H.C. Schultz-Coulon¹⁰, P. Schütz³, M. Schulz⁸, C. Schwick²⁷, J. Schwiening³, W.G. Scott²⁰, M. Settles¹²,
 T.G. Shears⁵, B.C. Shen⁴, C.H. Shepherd-Themistocleous⁷, P. Sherwood¹⁵, G.P. Siroti², A. Skillman¹⁵,
 A. Skuja¹⁷, A.M. Smith⁸, T.J. Smith²⁸, G.A. Snow¹⁷, R. Sobie²⁸, S. Söldner-Rembold¹⁰, R.W. Springer³⁰,
 M. Sproston²⁰, A. Stahl¹³, M. Starks¹², C. Stegmann¹⁰, K. Stephens¹⁶, J. Steuerer²⁸, B. Stockhausen³,
 D. Strom¹⁹, P. Szymanski²⁰, R. Tafiout¹⁸, H. Takeda²⁴, T. Takeshita²⁴, P. Taras¹⁸, S. Tarem²⁶, M. Tecchio⁹,
 P. Teixeira-Dias¹¹, N. Tesch³, J. Thomas³, M.A. Thomson⁸, O. Tousignant¹⁸, S. Towers⁶, M. Tscheulin¹⁰,
 T. Tsukamoto²⁴, A.S. Turcot⁹, M.F. Turner-Watson⁸, P. Utzat¹¹, R. Van Kooten¹², G. Vasseur²¹, P. Vikas¹⁸,
 M. Vincker²⁸, A. Wagner²⁷, D.L. Wagner⁹, C.P. Ward⁵, D.R. Ward⁵, J.J. Ward¹⁵, P.M. Watkins¹, A.T. Watson¹,
 N.K. Watson⁷, P. Weber⁶, P.S. Wells⁸, N. Vermes³, B. Wilkens¹⁰, G.W. Wilson²⁷, J.A. Wilson¹,
 V-H. Winterer¹⁰, T. Wlodek²⁶, G. Wolf²⁶, S. Wotton¹¹, T.R. Wyatt¹⁶, A. Yeaman¹³, G. Yekutieli²⁶, M. Yurko¹⁸,
 V. Zacek¹⁸, W. Zeuner⁸, G.T. Zorn¹⁷.

¹School of Physics and Space Research, University of Birmingham, Birmingham B15 2TT, UK

²Dipartimento di Fisica dell’ Università di Bologna and INFN, I-40126 Bologna, Italy

³Physikalisches Institut, Universität Bonn, D-53115 Bonn, Germany

⁴Department of Physics, University of California, Riverside CA 92521, USA

⁵Cavendish Laboratory, Cambridge CB3 0HE, UK

⁶Carleton University, Department of Physics, Colonel By Drive, Ottawa, Ontario K1S 5B6, Canada

- ⁷Centre for Research in Particle Physics, Carleton University, Ottawa, Ontario K1S 5B6, Canada
⁸CERN, European Organisation for Particle Physics, CH-1211 Geneva 23, Switzerland
⁹Enrico Fermi Institute and Department of Physics, University of Chicago, Chicago IL 60637, USA
¹⁰Fakultät für Physik, Albert Ludwigs Universität, D-79104 Freiburg, Germany
¹¹Physikalisches Institut, Universität Heidelberg, D-69120 Heidelberg, Germany
¹²Indiana University, Department of Physics, Swain Hall West 117, Bloomington IN 47405, USA
¹³Queen Mary and Westfield College, University of London, London E1 4NS, UK
¹⁵University College London, London WC1E 6BT, UK
¹⁶Department of Physics, Schuster Laboratory, The University, Manchester M13 9PL, UK
¹⁷Department of Physics, University of Maryland, College Park, MD 20742, USA
¹⁸Laboratoire de Physique Nucléaire, Université de Montréal, Montréal, Quebec H3C 3J7, Canada
¹⁹University of Oregon, Department of Physics, Eugene OR 97403, USA
²⁰Rutherford Appleton Laboratory, Chilton, Didcot, Oxfordshire OX11 0QX, UK
²¹CEA, DAPNIA/SPP, CE-Saclay, F-91191 Gif-sur-Yvette, France
²²Department of Physics, Technion-Israel Institute of Technology, Haifa 32000, Israel
²³Department of Physics and Astronomy, Tel Aviv University, Tel Aviv 69978, Israel
²⁴International Centre for Elementary Particle Physics and Department of Physics, University of Tokyo, Tokyo 113, and Kobe University, Kobe 657, Japan
²⁵Brunel University, Uxbridge, Middlesex UB8 3PH, UK
²⁶Particle Physics Department, Weizmann Institute of Science, Rehovot 76100, Israel
²⁷Universität Hamburg/DESY, II Institut für Experimental Physik, Notkestrasse 85, D-22607 Hamburg, Germany
²⁸University of Victoria, Department of Physics, P O Box 3055, Victoria BC V8W 3P6, Canada
²⁹University of British Columbia, Department of Physics, Vancouver BC V6T 1Z1, Canada
³⁰University of Alberta, Department of Physics, Edmonton AB T6G 2J1, Canada
³¹Duke University, Dept of Physics, Durham, NC 27708-0305, USA
³²Technische Hochschule Aachen, III Physikalisches Institut, Sommerfeldstrasse 26-28, D-52056 Aachen, Germany

^aAlso at TRIUMF, Vancouver, Canada V6T 2A3

^bRoyal Society University Research Fellow

1 Introduction

The Standard Model of electroweak and strong interactions has successfully passed the ever more rigorous tests that the accumulating LEP data have imposed [1]. Many searches have been carried out by OPAL and the other LEP detectors for new particles outside the Standard Model expectations but none has been successful [2]. Nevertheless, it is important to continue searching since there is a theoretical consensus that the Standard Model is not a complete theory [3].

An example of incompleteness of the theory is the presence of divergences, which may be removed by postulating higher symmetries such as Supersymmetry (SUSY). In SUSY, one anticipates the existence of a SUSY partner (sparticle) for every ordinary particle, boson or fermion, with identical couplings, and spin differing by half a unit [4, 5]. There is no experimental evidence so far for the existence of such sparticles, and searches at LEP and at $p\bar{p}$ colliders have placed stringent limits [5, 6, 7]. Examples of such sparticles are the gluinos, \tilde{g} — the spin 1/2 SUSY partners of the gluons — and the squarks, \tilde{q} — the scalar SUSY partners of quarks. We assume that a gluino could bind to a quark-antiquark pair to form a $(\tilde{g}q\bar{q}')$ state, or to a gluon to form a $(\tilde{g}g)$ state [8, 9]. All these states, if short-lived, would decay into the lightest SUSY particle, the neutralino, plus other particles. Short-lived gluinos have been excluded for masses smaller than $141 \text{ GeV}/c^2$ by experiments at Fermilab [10]. The possibility remains that gluinos and their charged compounds live long enough ($\sim 10^{-7}$ sec) to traverse the two-meter radius of the OPAL tracking chambers without decay. While many previous experiments have carried out searches for quasi-stable charged particles [9, 11, 12, 13], the

interpretation of these experiments remains somewhat controversial and model-dependent [13], so that different experimental approaches are of interest. In this paper we carry out the first search for such objects in Z^0 decays.

There is also a recurrent interest in looking for fractionally charged particles, such as unconfined quarks, produced in high energy collisions. The availability of large samples of events at LEP makes these searches particularly interesting.

In this paper we exploit the outstanding characteristics of the OPAL jet chamber to measure the specific ionization energy loss, dE/dx , of charged tracks [14]. Combining this information with a measurement of the momentum p of the particle allows a determination of the particle's mass, which in certain regions of dE/dx and p can be unique for a given particle's charge. We concentrate our attention on particles produced in Z^0 decays that have unusual charges ($Q/e = \pm 2/3, \pm 4/3, \pm 2$) or are heavier than a proton or antiproton and are singly-charged. We assume that these particles do not interact more strongly than normal hadrons, so that they can penetrate the small amount of matter ($\sim 1.5 \text{ g/cm}^2$) between the e^+e^- vertex and the first wire of the jet chamber without interaction or decay. One example of such a particle would be a charged bound state $(\tilde{g}q\bar{q}')^\pm$ containing a neutral gluino bound to a charged quark-antiquark pair. Another example within the Standard Model would be an (anti)deuteron or (anti)triton decay particle from the Z^0 . These are expected to be rare; they have been observed in earlier e^+e^- searches [15] at lower energies, but in $\Upsilon(1S)$ decays only.

The search described in this paper examines the multi-hadronic and the low-charged multiplicity Z^0 decay event samples collected with the OPAL detector at LEP in the years 1991–1993.

2 The OPAL Detector

The OPAL detector has been described in detail elsewhere [16]. It is a multipurpose detector covering almost the entire solid angle around the interaction region at LEP. Its main parts are a system of central tracking chambers and a silicon microvertex detector inside a magnetic field of 0.435 T, an electromagnetic calorimeter, a hadron calorimeter and an outer shell of muon chambers.

The tracking chambers are the main tool for this analysis. Three sets of chambers allow an accurate determination of the vertex of the interaction and of charged particle momenta. The chamber closest to the beam is the vertex chamber that measures space coordinates with accuracies of $\sigma_{r\phi} \approx 50 \mu\text{m}$ and $\sigma_z \approx 700 \mu\text{m}$.¹ The main part of the tracking system is a jet chamber about 2 m in radius and 4 m in length. It is divided into 24 sectors, each equipped with 159 layers of sense wires. Up to 159 measurements per track are possible with a precision of $\sigma_{r\phi} \approx 135 \mu\text{m}$ and $\sigma_z \approx 6 \text{ cm}$. A precise measurement of the z -coordinate is provided by a set of drift chambers (Z-chambers) located at a radius of 192 cm from the beam line yielding up to six measurements each with a resolution of $\sigma_z \approx 300 \mu\text{m}$. The combination of these chambers leads to a momentum resolution of $\sigma_{p_t}/p_t \approx \sqrt{0.02^2 + (0.0015 \cdot p_t)^2}$ (p_t , in GeV/c , is the momentum transverse to the beam direction); the first term represents the contribution from multiple scattering.

Particles are identified by the simultaneous measurement of momentum p and energy loss dE/dx in the jet chamber (Fig. 1). A detailed description of the energy loss measurement can be found in Ref. [14]. The typical resolution achieved in multi-hadronic events is $\sigma(dE/dx)/(dE/dx) = 3.5\%$ for 159 charge samples on a track. The points shown in Fig. 1 are obtained from a subset of multi-hadronic events. Clear separations between π , K, p and d particles are seen for $dE/dx \geq 12 \text{ keV/cm}$. Theoretical ionization curves are also shown for a particle with $|Q/e| = 1$ and mass $M = 10 \text{ GeV}/c^2$, and with $|Q/e| = 2/3$ and $M = 0.1 \text{ GeV}/c^2$. The strength of the dE/dx system is illustrated in OPAL's detailed analysis of π , K and p production in Z^0 multi-hadronic decays [17].

¹ A right-handed coordinate system is adopted by OPAL where the x axis points to the centre of the LEP ring, and positive z is along the electron beam direction. The angles θ and ϕ are the polar and azimuthal angles, respectively.

3 Event and Track Selection

The data examined in this analysis correspond to an integrated luminosity of about 74 pb^{-1} collected in 1991–1993. Using the standard OPAL multi-hadronic event selection [18], 1.64×10^6 events remain. This selection accepts $(98.4 \pm 0.4)\%$ of multi-hadronic events. Backgrounds in this sample, such as $e^+e^- \rightarrow \tau^+\tau^-$, beam-gas and $\gamma\gamma$ interactions are estimated to be at a level of about 0.2%.

Tracks are required to have a minimum transverse momentum relative to the beam direction of $0.15 \text{ GeV}/c$. They are accepted if their distance of closest approach to the common event vertex in the plane transverse to the beam direction is less than 1 cm ($|d_0| < 1 \text{ cm}$) and if their distance from the nominal interaction point along the beam direction at the distance of closest approach is less than 40 cm ($|z_0| < 40 \text{ cm}$). This reduces, but does not eliminate completely, the number of tracks from nuclear interactions in the detector material.

For each track a minimum of 100 hits in the jet chamber usable for the determination of the energy loss dE/dx are required. A match of the track to hits in the Z-chambers and hits in the vertex chambers is also required. The first condition assures an overall dE/dx resolution of about 4.0% for tracks in multi-hadronic events. The second condition is applied in order to obtain a good resolution of the polar angle θ . Since the Z-chambers cover the barrel region only, the acceptance is restricted to $|\cos\theta| < 0.7$. A further cut on χ^2 is applied to the track fit in the r - ϕ plane, which rejects roughly 5% of the tracks with large values of χ^2 in the distribution. Comparing the number of charged particles retained in our sample with these conditions to the average number of charged primary particles produced per event (charged multiplicity of (21.40 ± 0.43) [19]), we determine a track retention efficiency of $(19.7 \pm 0.4)\%$ for tracks of positive charge, $(23.4 \pm 0.5)\%$ for tracks of negative charge, where the errors are mainly due to the error on the charged multiplicity. The difference between the two quoted efficiencies is due to Lorentz angle effects in the jet chamber, which cause the negatively-charged tracks to have on average more hits than the positively-charged ones [20, 21]. The average track efficiency is $(21.5 \pm 0.5)\%$, including geometrical acceptance, track quality and dE/dx determination.

4 Ionization Energy Loss Measurements

In Fig. 2(a) we show the observed ionization energy loss measurements in units of keV/cm versus momentum for positively-charged tracks from our entire multi-hadronic sample that are at least four standard deviations above or five standard deviations below the expected values for protons, pions, kaons or positrons; the asymmetry of this cut is due to the presence of many pions at lower dE/dx values. A clear signal is seen for deuterons and tritons (at masses $M_d = 1.876 \text{ GeV}/c^2$ and $M_t = 2.82 \text{ GeV}/c^2$, respectively) which come from the fragmentation of nuclei in beam-gas and beam-wall interactions (notice that these processes do not yield antideuterons nor antitritons). These tracks cluster along the expected theoretical dE/dx curves and indicate that this method of determining a particle's mass from its momentum and dE/dx can indeed be experimentally carried out in the OPAL detector. Figure 2(b) shows the same measurements for negatively-charged tracks where only one antideuteron candidate (labeled (1) in Fig. 2(b)) and no antitriton candidate are seen. Another phenomenon observed in Figs. 2(a,b) is the band of tracks with dE/dx close to twice the expected ionization rate for relativistic electrons, pions, kaons and protons (15 – $24 \text{ keV}/\text{cm}$). These entries are attributed to pairs of tracks with the same charge, that are so close to each other in angle and momentum that they are reconstructed by the detector as one track with twice the usual ionization loss. This phenomenon is reproduced by the standard OPAL multi-hadronic Monte Carlo simulation [22, 23]. In our search for heavy stable particles with $|Q/e| = 1$, we shall limit the search area to directly produced charged particles with mass heavier than a proton (triton), if negative (positive), and with an ionization loss $dE/dx \geq 25 \text{ keV}/\text{cm}$. This latter value is chosen to eliminate the double tracks described above. Only one negatively-charged candidate track for particles heavier than a triton was found. The search for directly produced deuterons or antideuterons will be limited to negative tracks, since too many secondary deuterons are produced by nuclear interaction of the lighter hadrons before they reach the central tracking detector.

5 Search for Negatively-Charged Heavy Stable Particles

In Fig. 2(b) we show the ionization energy loss versus momentum for negatively-charged particles with $dE/dx \geq 25$ keV/cm that might correspond to masses greater than the mass of the antiproton. Five tracks, labeled (1)–(5) in Fig. 2(b), were found in or near the search region. Track (1) is at first inspection consistent with an antideuteron with an ionization energy loss of 60 keV/cm and a momentum of 670 MeV/c, corresponding to a mass of (2.0 ± 0.1) GeV/ c^2 , where the error is due to the errors on the measurements of dE/dx and p . A more detailed analysis shows that the track does not come from the primary vertex, since $z_0 \simeq 27$ cm; on the basis of increasing curvature and increasing dE/dx , we conclude that this track is produced by a positively-charged deuteron produced outside the tracking chamber by a nuclear interaction, and subsequently travelling inwards across the whole jet chamber. Track (2), with dE/dx equal to 39 keV/cm and momentum 1.8 GeV/c, would be consistent with a singly-charged particle of mass (4.2 ± 0.1) GeV/ c^2 . Time of flight information does not give further discrimination. In the mass region greater than the mass of the deuteron, there is one other track (3) with $dE/dx = 26.0$ keV/cm and a momentum $p = 12.5$ GeV/c that is compatible with two overlapping electrons of almost equal momenta, since the observed electromagnetic energy associated to the track is twice the observed momentum: the energy released in the electromagnetic cluster associated to the track is 25.0 GeV and there are no other tracks associated to this cluster. In the mass region below 1.5 GeV/ c^2 there are two further candidate tracks: one (4) with $dE/dx = 58.0$ keV/cm and $p = 0.40$ GeV/c is clearly a double track when viewed in a graphic display — it splits into two tracks at large radius — and the second (5) with $dE/dx = 25.4$ keV/cm and $p = 0.81$ GeV/c has an ionization compatible with an antiproton track overlapping an electron track.

A detailed Monte Carlo analysis based on the event generator JETSET 7.3 [22] and the detector simulation program GOPAL/GEANT [23] has been carried out with 980,000 multi-hadronic events. In the mass region $M > 3$ GeV/ c^2 it predicts one negative and one positive track with an ionization greater than our cutoff of 25 keV/cm, or 1.7 events of each sign in a sample scaled to our data set. One of the two background tracks is a π^- overlapping a K^- . The other one is a π^+ with five δ -rays associated. Although the Monte Carlo statistics are low, the negatively-charged candidate track found in the data at a mass of 4.2 GeV/ c^2 can be compatible with background. The Monte Carlo is not reliable for predicting the number of deuterons and tritons produced in secondary interactions since the simulation of such nuclear interactions is not correctly tuned in the present simulation program GEANT [23].

We can deduce 95% confidence level (C.L.) upper limits for the probability w of new particle production according to the formula:

$$w < \frac{N_{sup}}{N_{MH} \times (\epsilon - \sigma_\epsilon)},$$

where N_{sup} is 3.00 for zero candidates, 4.74 for one candidate; N_{MH} is the number of processed multi-hadronic events; ϵ is the detection efficiency and σ_ϵ its uncertainty. The upper limits for antideuteron and antitriton production (for which we have no candidates) in specific ranges of momentum in $e^+e^- \rightarrow$ hadrons events at $\sqrt{s} \simeq M_{Z^0}$ are:

$$w(0.35 \text{ GeV}/c < p_{\bar{d}} < 1.1 \text{ GeV}/c) < 0.8 \times 10^{-5}$$

and

$$w(0.5 \text{ GeV}/c < p_{\bar{t}} < 1.6 \text{ GeV}/c) < 0.8 \times 10^{-5},$$

respectively.

A model for antideuteron production, described in Ref. [24], predicts a total antideuteron rate of $w \approx 5 \times 10^{-5}$ per multi-hadronic event at LEP energies. In the momentum range of 0.35–1.1 GeV/c accepted by this experiment the prediction is $w \approx 0.3 \times 10^{-5}$.

A previous report on the direct production of antideuterons in e^+e^- collisions, made by ARGUS [15] at DORIS, at the $\Upsilon(1S)$ peak, gave a probability of antideuteron production over the whole momentum range, of $w = (6.0 \pm 2.0 \pm 0.6) \times 10^{-5}$ from Υ decays, and a 90% C.L. upper limit of $w < 1.7 \times 10^{-5}$ from $e^+e^- \rightarrow \gamma^* \rightarrow q\bar{q}$ events.

6 Comparison of the $|Q/e| = 1$ Heavy Particle Search with Estimates of Gluino Charged Bound State Production

In this section we compare the experimental results described above with what might be expected if light gluinos were produced and could emerge from the Z^0 vertex as quasi-stable charged colorless $(\tilde{g}q\bar{q}')^\pm$ bound states.

To estimate the possible gluino production rate as a function of gluino mass, we use the differential cross section calculation and program generator of Muñoz-Tapia and Stirling [25] for the reaction $e^+e^- \rightarrow q\bar{q}\tilde{g}\tilde{g}$. To take into account the gluino fragmentation process, we assume that a $5 \text{ GeV}/c^2$ gluino will fragment in the same manner as a $5 \text{ GeV}/c^2$ b-quark using a Peterson fragmentation function [26] with parameter $\epsilon_b = 0.0055$ [27]. For other mass values of the gluino we scale the ϵ -parameter by the factor $(M_{\tilde{g}}/(5 \text{ GeV}/c^2))^{-2}$. A Monte Carlo calculation that folds the production cross section with the fragmentation function was then carried out to determine how many gluino candidates would be produced in 1.64×10^6 multi-hadronic events, with the gluino emitted in the angular region $|\cos\theta| \leq 0.7$ and with the momentum of the dressed gluino state low enough to produce an ionization loss greater than $25 \text{ keV}/\text{cm}$ (if charged). We assume that the masses of dressed gluino states are equal to the mass of the gluino $M_{\tilde{g}}$. The results of this calculation for various values of $M_{(\tilde{g}q\bar{q}')^\pm}$ are shown in the second column of Table I.

In the fragmentation process, a quasi-stable gluino has to form a colorless bound state. This can be achieved by attaching one or more gluons, or another gluino, or a color-octet $q\bar{q}'$ system to the gluino, resulting in the so-called glueballino, gluinoball, or neutral or charged SUSY-hybrid $(\tilde{g}q\bar{q}')$ compound, respectively. To observe the charged $(\tilde{g}q\bar{q}')^\pm$ compounds, some of them have to be sufficiently long-lived to traverse the OPAL jet chamber without decaying. This can happen if they are close enough in mass to the lightest neutral gluino bound states (the mass difference being $\Delta M < M_\pi$) so that they will not decay rapidly to a neutral gluino bound state and a charged pion. This assumption has been discussed theoretically in Ref. [8], where the expected charged to neutral mass differences have been estimated to lie in the range $[-20 \text{ MeV}/c^2, +40 \text{ MeV}/c^2]$ for spin-1/2 gluino ρ -like and π -like states, respectively.

The fraction, P_Q , of charged quasi-stable $(\tilde{g}q\bar{q}')^\pm$ states emerging from gluino fragmentation is not known. If we assume that gluino fragmentation leads only to quasi-stable gluino bound states of the gluino-quark-antiquark type $(\tilde{g}q\bar{q}')$, and that the charged gluino-quark-antiquark states $(\tilde{g}q\bar{q}')^\pm$ do not decay into the lightest neutral gluino bound states, whose relative masses are unknown, in times less than $\sim 10^{-7}$ sec, then one would expect $P_Q \sim 50\%$ since there would be an equal number of charged and neutral configurations, analogous to π^+ , π^- , π^0 and η^0 . If gluino-gluon states are also allowed, they might be produced roughly 50% of the time, so that $P_Q \sim 25\%$. The production of gluinoballs $(\tilde{g}\tilde{g})$ would further reduce this fraction, but is expected not to be sizeable. In the following discussion we quote limits for both $P_Q = 25\%$ and $P_Q = 50\%$.

In columns 3 and 4 of Table I we list the expected number of $(\tilde{g}q\bar{q}')^\pm$ tracks obtained by multiplying the number of gluinos produced by the assumed probability (25% and 50% respectively) of emerging charged and by the average efficiency $(35.5 \pm 3.0)\%$ for satisfying all the criteria listed in our track selection in Sect. 3 other than $|\cos\theta| \leq 0.7$. The combined multiplication factor is 0.09 and 0.18 respectively, and yields the numbers listed in columns three and four. Since only one clear candidate was observed among the negative tracks and zero among the positive tracks, we can provide limits for quasi-stable $(\tilde{g}q\bar{q}')^\pm$ states. Assuming $P_Q = 25\%$, the 95% C.L. lower limit for the mass of a charged, quasi-stable $(\tilde{g}q\bar{q}')^\pm$ state is $13.6 \text{ GeV}/c^2$ after reducing the expected numbers in column three by one standard deviation of the total estimated error (about 10%, coming from 3% due to Monte Carlo event statistics, 4% from fragmentation, 3% from tracking geometry and dE/dx determinations, 2% from the average multiplicity of multi-hadronic events, and 7 to 8% from systematics in theoretical modeling of gluino production). If $P_Q = 50\%$, the lower limit for the $(\tilde{g}q\bar{q}')^\pm$ mass is $16.6 \text{ GeV}/c^2$.

In the mass region $1.2 \text{ GeV}/c^2 < M_{(\tilde{g}q\bar{q}')^\pm} < 4 \text{ GeV}/c^2$, the search is confined to negative particles because of the large number of background deuterons and tritons produced in secondary nuclear interactions. For this reason, the expected values in columns 3 and 4, first three rows of Table I have been halved. Overall, this search excludes a quasi-stable charged gluino in the mass region $1.9 - 13.6 \text{ GeV}/c^2$ at the 95% confidence level, given our assumption as to the frequency of charged quasi-stable gluino compound formation of 25%; if $P_Q = 50\%$, the excluded mass range extends to $1.2 - 16.6 \text{ GeV}/c^2$.

If some of the charged $(\tilde{g}q\bar{q}')^\pm$ states can decay strongly into the lightest neutral gluino bound state, or if $(\tilde{g}g)$ production is favoured with respect to $(\tilde{g}q\bar{q}')$ production in the fragmentation process, our estimates on P_Q would have to be lowered. Thus we give in the last column of Table I the estimated upper limits on P_Q dependent on the $(\tilde{g}q\bar{q}')^\pm$ mass. One observes that our analysis is sensitive down to P_Q of about 6% for certain mass values.

Table I - Monte Carlo calculation of the number of gluinos expected in 1.64×10^6 multi-hadronic events.

Notice that for $M_{(\tilde{g}q\bar{q}')^\pm} < 4 \text{ GeV}/c^2$ (first three rows, values marked with asterisks) only negative tracks are used — see text. The number of charged tracks scales with P_Q . The last column gives the resulting upper limit on P_Q .

$M_{\tilde{g}} \simeq M_{(\tilde{g}q\bar{q}')^\pm}$ (GeV/ c^2)	Number of \tilde{g} -compounds ($ \cos\theta \leq 0.7$; $dE/dx > 25 \text{ keV/cm}$)	Number of expected $(\tilde{g}q\bar{q}')^\pm$ tracks		P_Q upper limit (95% C.L.)
		$P_Q = 25\%$	$P_Q = 50\%$	
1.5	79.9	3.5*	7.1*	36.7% *
2.3	147.3	6.5*	13.1*	19.9% *
3.0	205.9	9.1*	18.3*	14.2% *
5.0	238.3	21.2	42.3	6.1%
10.0	114.9	10.2	20.4	12.7%
15.0	43.9	3.9	7.8	33.4%
20.0	14.2	1.3	2.5	103.2%

Null results for stable gluino bound states have been obtained previously by other kinds of experiments with different theoretical assumptions in similar mass ranges, as described in [9, 12] and in [13, p. 1803]. A negative search for massive particles at the Z^0 peak, using a smaller event sample, has previously been carried out by ALEPH [28] at LEP. CDF [29] has carried out a negative search for massive quasi-stable charged particles produced in $p\bar{p}$ collisions for a mass range larger than $50 \text{ GeV}/c^2$. Finally, OPAL has carried out a negative search for isolated neutral massive particles produced at LEP [30] and a negative search for Z^0 decays into a pair of singly-charged heavy stable particles [31].

7 Search for Particles with Anomalous Charge and/or Mass

As can be seen in Fig. 1 relativistic charged particles with $|Q/e| = 2/3$ would ionize at a rate of $3 - 4 \text{ keV/cm}$, much below the ionization rate for integer charged particles. Particles with $|Q/e| = 2/3$ and with masses larger than $0.1 \text{ GeV}/c^2$ — the example shown in Fig. 1 — would have dE/dx curves shifted to higher momenta but with similar small values for dE/dx . The search for $|Q/e| = 2/3$ particles is not restricted to the narrow momentum region in which dE/dx is steeply rising, but also covers the much broader relativistic momentum region. We do not consider for the moment the search for $|Q/e| = 1/3$ particles, because their ionization energy loss, which is $1/9$ of that of ordinary particles, is too close to the threshold for charge to register hits in the jet chamber.

From an analysis of the dE/dx distribution for the singly-charged particles, it has been noted that in the low dE/dx region, 3σ below the mean, the dE/dx spectrum is non-gaussian. As a consequence, there is an excess of tracks over what is expected for the 5σ cut off. For this reason, the search has been restricted to $dE/dx < 4 \text{ keV/cm}$, which is still sensitive to almost all the fast $|Q/e| = 2/3$ particles. This cut off line is raised at high p , as shown in Figs. 2(a,b), to take into account the relativistic rise of the dE/dx curves, and the fact that in this momentum region such background is smaller. Only one candidate is left, with $dE/dx = 3.87 \text{ keV/cm}$ and a mass of about $1.7 \text{ GeV}/c^2$, assuming $|Q/e| = 2/3$ (see Fig. 2(a)). The inner part of this track looks just like a singly-charged minimum-ionizing track (dE/dx samples at about 7 keV/cm), while in the most external region the measured dE/dx drops down to about 3 keV/cm . However, a second track close to the candidate track shows a drop of similar size in the measured dE/dx , giving a strong indication of a deterioration of the dE/dx measurement for these tracks. The explanation was found in a very large space charge from a highly ionizing low momentum track causing a temporary reduction of the amplification.

The efficiency of recording a $|Q/e| = 2/3$ track is found to be 96.5% of that of a $|Q/e| = 1$ track [20]; this estimate was obtained by reducing the gas pressure in the tracking chamber, in order to emulate charged tracks with $|Q/e| < 1$. Thus, the overall detection efficiency for the tracks accepted in our sample is $(20.7 \pm 0.5)\%$. This implies a 95% C.L. upper limit for $|Q/e| = 2/3$ particles in the observable momentum region (for quark masses greater than $2 \text{ GeV}/c^2$) of

$$w(p > 3.5 \text{ GeV}/c) < 0.9 \times 10^{-5}$$

for unconfined quarks per multi-hadronic Z^0 decay.

A more detailed estimate of the average detection efficiency over the whole momentum range, taking into account the accepted regions in the dE/dx versus p plot, was carried out using a standard multi-hadronic Monte Carlo, adding a $|Q/e| = 2/3$ particle to each event [21]. On the phase space distribution for these ‘unconfined quarks’ two hypotheses were made: (i) equal to that of ordinary colorless hadrons; (ii) such that $E \frac{dN}{d^3p} = \text{constant}$. As a result one can obtain a ratio of free quark production to multi-hadronic production. This ratio is shown, as a function of particle mass, in Fig. 3, according to the two different hypotheses on phase space. The comparison of our limits with other e^+e^- searches (see [13, p. 1791] and [28, 32]) is displayed in Fig. 4. Here, for consistency with previous publications, the limits are at the 90% confidence level, the phase space distribution is assumed to be such that $E \frac{dN}{d^3p} = \text{constant}$ and the rate for free quark production is given relative to the $e^+e^- \rightarrow \mu^+\mu^-$ event rate.

Similar searches were carried out for $|Q/e| = 1, 4/3$ and 2 in the high ionization region ($dE/dx > 25 \text{ keV}/\text{cm}$). Only one candidate was found for tracks that satisfied our strict selection criteria. This is the track already discussed in Section 5 corresponding to a mass of $4.2 \text{ GeV}/c^2$ for $Q/e = -1$. For these conjectured particles we use the same efficiency and angular distribution as for normal particles with $|Q/e| = 1$, namely $(21.5 \pm 1.9)\%$. In the appropriate momentum interval for each assumed mass this yields a 95% confidence level upper limit per multi-hadronic event, for particles with $|Q/e| = 4/3$, of

$$w(\text{allowed } p - \text{range}) < 1.4 \times 10^{-5}.$$

The same limit holds for particles with $|Q/e| = 2$. Again, with the same assumptions for the momentum distribution of these particles, one can calculate limits for the ratio of such anomalous particle cross sections to the multi-hadronic production cross sections as a function of particle mass; the results are shown in Fig. 3.

8 Search in Low Charged Multiplicity Events

We have extended the search described for multi-hadronic events, to cover also the events characterised by a low charged multiplicity. The low multiplicity data sample consists of 1.8×10^6 events collected from 1991 to 1993. The selection requires the events to contain at least one, but less than 18, good charged tracks and/or good electromagnetic clusters; for each track a minimum transverse momentum (relative to the beam direction) of $700 \text{ MeV}/c$ is required. It contains e^+e^- , $\mu^+\mu^-$ and $\tau^+\tau^-$ final states, events due to two-photon collisions, beam-gas interactions and overlaps with the multi-hadronic event data sample.

In this analysis the same quality cuts, as described in the analysis of multi-hadronic events, are applied to the tracks. Again, the phenomenon of overlapping tracks is observed. Secondary deuterons and tritons, but no antideuterons nor antitritons, are detected. The deuteron and triton tracks come mainly from beam-gas interactions. The search for new particles was carried out both in the region of high ionization and of low ionization, as indicated in Figs. 5(a,b). Because of the lower background, such regions are generally wider than those indicated in Figs. 2(a,b). No candidate track was found out of the entire sample.

In order to set limits which are independent of, and complementary to those derived from the search in multi-hadronic events, we consider only the back-to-back production of pairs of new stable charged particles in two-prong events. This yields the following 95% C.L. limits for the number of new-particle pairs relative to the number of muon pairs ($N_{\mu^+\mu^-} = 78\,700$) in our data sample:

$$\text{free quarks with } |Q/e| = 2/3 \text{ and } M_q < 37 \text{ GeV}/c^2 \text{ or } 43.6 \text{ GeV}/c^2 < M_q < 45.6 \text{ GeV}/c^2: \frac{N_{q\bar{q}}}{N_{\mu^+\mu^-}} < 1.9 \times 10^{-4}$$

$$\left. \begin{array}{l} \text{particles with } |Q/e| = 1 \text{ and } 40.4 \text{ GeV}/c^2 < M_x < 45.6 \text{ GeV}/c^2 \\ \text{particles with } |Q/e| = 4/3 \text{ and } M_x < 0.1 \text{ GeV}/c^2 \text{ or } 35.1 \text{ GeV}/c^2 < M_x < 45.6 \text{ GeV}/c^2 \\ \text{particles with } |Q/e| = 2 \text{ and } M_x < 45.6 \text{ GeV}/c^2 \end{array} \right\} \frac{N_{x\bar{x}}}{N_{\mu^+\mu^-}} < 1.8 \times 10^{-4}$$

where the mass ranges are dictated by the search region and by the fact that in back-to-back production the momentum is fixed by the assignment of the particle's mass.

9 Summary and Conclusions

A search has been carried out in a sample of 1.64×10^6 Z^0 multi-hadronic decays and in a low charged multiplicity event sample for two types of unusual particles: (i) singly-charged particles with masses larger than $3 \text{ GeV}/c^2$ and for negative, singly-charged particles in the mass region $1.2 - 4.0 \text{ GeV}/c^2$ and (ii) charged particles with $|Q/e| = 2/3, 4/3$ and 2 .

In search (i), one candidate particle of mass $4.2 \text{ GeV}/c^2$ was found, which is consistent with background. No antideuteron nor antitriton candidates were found, hence the 95% C.L. upper limit for the probability of antideuteron and/or antitriton production in the search region is 0.8×10^{-5} . For the integer charged particles our experimental results were compared to the expected production in $e^+e^- \rightarrow q\bar{q}\tilde{g}\tilde{g}$ reactions assuming that a gluino can emerge as a quasi-stable charged $(\tilde{g}q\bar{q}')^\pm$ state. We have determined limits on the fraction P_Q of such states emerging in the gluino fragmentation process, depending on their mass. If we assume $P_Q = 25\%$, we can rule out quasi-stable $(\tilde{g}q\bar{q}')^\pm$ states in the mass region $1.9 \text{ GeV}/c^2 < M_{\tilde{g}} < 13.6 \text{ GeV}/c^2$ at the 95% C.L. If $P_Q = 50\%$, the excluded mass region becomes $1.2 - 16.6 \text{ GeV}/c^2$.

No evidence was found for anomalously charged particles that might be generated by free quarks or particles with higher charge and 95% C.L. limits are presented, from both the multi-hadronic and the low-multiplicity samples.

10 Acknowledgements:

It is a pleasure to thank the SL Division for the efficient operation of the LEP accelerator, the precise information on the absolute energy, and their continuing close cooperation with our experimental group. In addition to the support staff at our own institutions we are pleased to acknowledge the

Department of Energy, USA,
National Science Foundation, USA,
Particle Physics and Astronomy Research Council, UK,
Natural Sciences and Engineering Research Council, Canada,
Fussefeld Foundation,
Israel Ministry of Science,
Israel Science Foundation, administered by the Israel Academy of Science and Humanities,
Minerva Gesellschaft,
Japanese Ministry of Education, Science and Culture (the Monbusho) and a grant under the Monbusho International Science Research Program,
German Israeli Bi-national Science Foundation (GIF),
Direction des Sciences de la Matière du Commissariat à l'Energie Atomique, France,
Bundesministerium für Forschung und Technologie, Germany,
National Research Council of Canada,
A.P. Sloan Foundation and Junta Nacional de Investigação Científica e Tecnológica, Portugal.

We also thank J. Ellis and F. Zwirner for discussions.

Figures

- Fig. 1** Observed energy loss versus momentum for all ‘good’ positively- and negatively-charged tracks in a sample of about 10,000 multi-hadronic events.
- Fig. 2** (a) Observed ionization loss in units of keV/cm versus momentum for positively-charged ‘good’ tracks from the entire multi-hadronic sample that are at least four standard deviations above or five standard deviations below the expected values for pions, kaons, protons and positrons. The excluded region for typical dE/dx errors is shaded. The outer boundary (bold line) delimits the search region. (b) The same as in (a), but for negatively-charged ‘good’ tracks.
- Fig. 3** 95% C.L. upper limits for the production of charged stable particles with $|Q/e| = 1, 2/3, 4/3, 2$. In the vertical scale is plotted the ratio $R_X = \sigma(e^+e^- \rightarrow X + \text{hadrons}) / \sigma(e^+e^- \rightarrow \text{hadrons})$, where X is the particle searched for. Two models are considered for the phase space distribution: (i) the same as for normal hadrons (continuous lines); (ii) such that $E \frac{dN}{d^3p} = \text{constant}$ (dashed lines).
- Fig. 4** Compilation of 90% C.L. upper limits for the production of particles with $|Q/e| = 2/3$. The quoted searches have been described in Refs. [28, 32]. The phase space distribution is assumed to be such that $E \frac{dN}{d^3p} = \text{constant}$.
- Fig. 5** (a) Observed ionization loss in units of keV/cm versus momentum for positively-charged ‘good’ tracks from the low-multiplicity sample that are at least four standard deviations above or five standard deviations below the expected values for pions, kaons, protons and positrons. The excluded region for typical dE/dx errors is shaded. The outer boundary (bold line) delimits the search region. The deuteron and triton tracks come mainly from beam-gas interactions. (b) The same as in (a), but for negatively-charged ‘good’ tracks.

References

- [1] D. Schaile, “Precision Tests of the Electroweak Interaction”, Int. Conf. on High Energy Physics, Glasgow, CERN-PPE/94-162 (1994).
- [2] M. Pohl, “Search for New Particles and New Interactions”, Int. Conf. on High Energy Physics, Glasgow (1994).
- [3] See for example: S. Weinberg, “Dreams of a Final Theory”, Pantheon Books (1993).
- [4] P. Fayet, Phys. Lett. **B69** (1977) 489;
R. Barbieri, Riv. Nuovo Cimento 11 (1988) 4;
F. Zwirner, “The SUSY World” – 1993, Proceedings, Ed. by L. Cifarelli, V. A. Khoze and A. Zichichi, World Sci., Singapore (1993) 509.
- [5] Proceedings of the Workshop “Ten years of SUSY confronting experiments”, CERN 7–9 September 1992.
- [6] G. Giacomelli and P. Giacomelli, Riv. Nuovo Cimento 16 (1993) 1.
- [7] J. Ellis *et al.*, Phys. Lett. **B262** (1991) 109;
J. Ellis *et al.*, Phys. Lett. **B305** (1993) 375.
- [8] M. Chanowitz and S. Sharpe, Phys. Lett. **B126** (1983) 225.
- [9] G. R. Farrar, RU-94-35 (1994).
- [10] CDF Coll., F. Abe *et al.*, Phys. Rev. Lett. **69** (1992) 3439.
- [11] G. R. Farrar, Phys. Rev. Lett. **53** (1984) 1029;
S. Dawson *et al.*, Phys. Rev **D31** (1985) 1581.
- [12] UA1 Coll., C. Albajar *et al.*, Phys. Lett. **B198** (1987) 261.
- [13] L. Montanet *et al.*, Review of Particle Properties, Phys. Rev. **D50** (1994) 3-I.
- [14] M. Hauschild *et al.*, Nucl. Instr. Meth. **A314** (1992) 74.
- [15] ARGUS Coll., H. Albrecht *et al.*, Phys. Lett. **B236** (1990) 102.
- [16] OPAL Coll., K. Ahmet *et al.*, Nucl. Instr. Meth. **A305** (1991) 275.
- [17] OPAL Coll., R. Akers *et al.*, Z. Phys. **C63** (1994) 181.
- [18] OPAL Coll., G. Alexander *et al.*, Z. Phys. **C52** (1991) 175.
- [19] OPAL Coll., P. D. Acton *et al.*, Z. Phys. **C53** (1992) 539.
- [20] J. Thomas, “Suche nach freien Quarks in multihadronischen Zerfällen des Z^0 ”, Diplomarbeit, Physics Dept., University of Bonn, BONN-IR-93-13 (1993).
- [21] M. Fanti, “Studio del Fondo Indotto dai Fasci di LEP e Ricerca di Particelle a Ionizzazione Anomala”, Tesi di Laurea, Physics Dept., University of Bologna, Tesi n. 1890 (1994).
- [22] T. Sjöstrand “PYTHIA 5.6 and JETSET 7.3: Physics and Manual”, CERN-TH 6488/92 (1992).
- [23] J. Allison *et al.*, Nucl. Instr. Meth. **A317** (1992) 47;
GEANT Detector Description and Simulation Tool, CERN Program Library Long Writeup W5013 (1993).
- [24] G. Gustafson *et al.*, Z. Phys. **C61** (1994) 683.
- [25] R. Muñoz-Tapia and W. J. Stirling, Phys. Rev. **D49** (1994) 3763.
- [26] C. Peterson *et al.*, Phys. Rev. **D27** (1983) 105.
- [27] OPAL Coll., R. Akers *et al.*, Z. Phys. **C60** (1993) 199.
- [28] ALEPH Coll., D. Buskulic *et al.*, Phys. Lett. **B303** (1993) 198.

- [29] CDF Coll., F. Abe *et al.*, Phys. Rev. Lett. **63** (1989) 1447.
- [30] OPAL Coll., P. D. Acton *et al.*, Phys. Lett. **B278** (1992) 485.
- [31] OPAL Coll., M. Z. Akrawy *et al.*, Phys. Lett. **B252** (1990) 290.
- [32] JADE Coll., W. Bartel *et al.*, Z. Phys. **C6** (1980) 295;
TPC/PEP4 Coll., H. Aihara *et al.*, Phys. Rev. Lett. **52** (1984) 2332;
ARGUS Coll., H. Albrecht *et al.*, Phys. Lett. **B156** (1985) 134;
CLEO Coll., T. Bowcock *et al.*, Phys. Rev. **D40** (1989) 263;
TOPAZ Coll., I. Adachi *et al.*, Phys. Lett. **B244** (1990) 352.

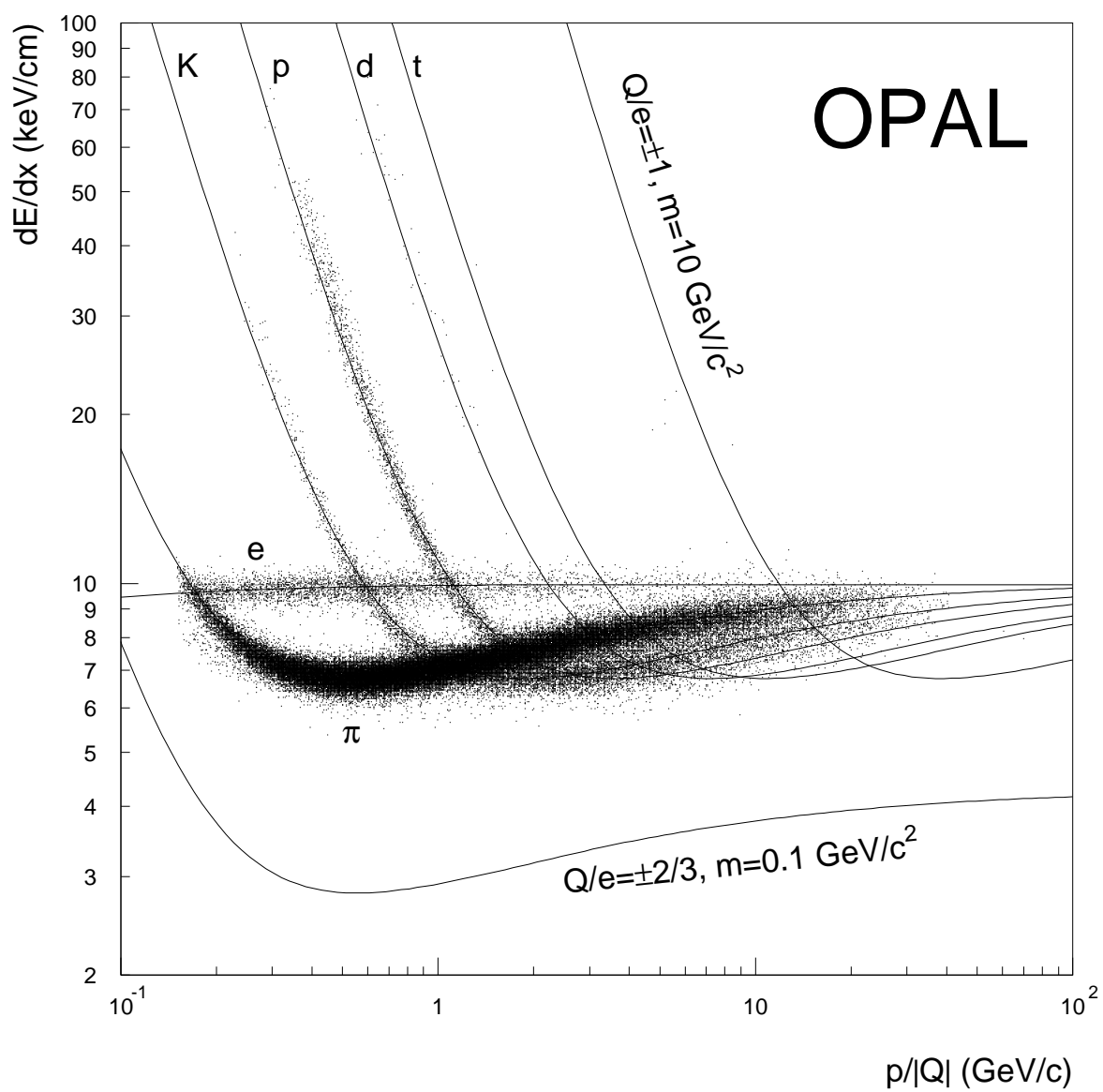


Fig. 1

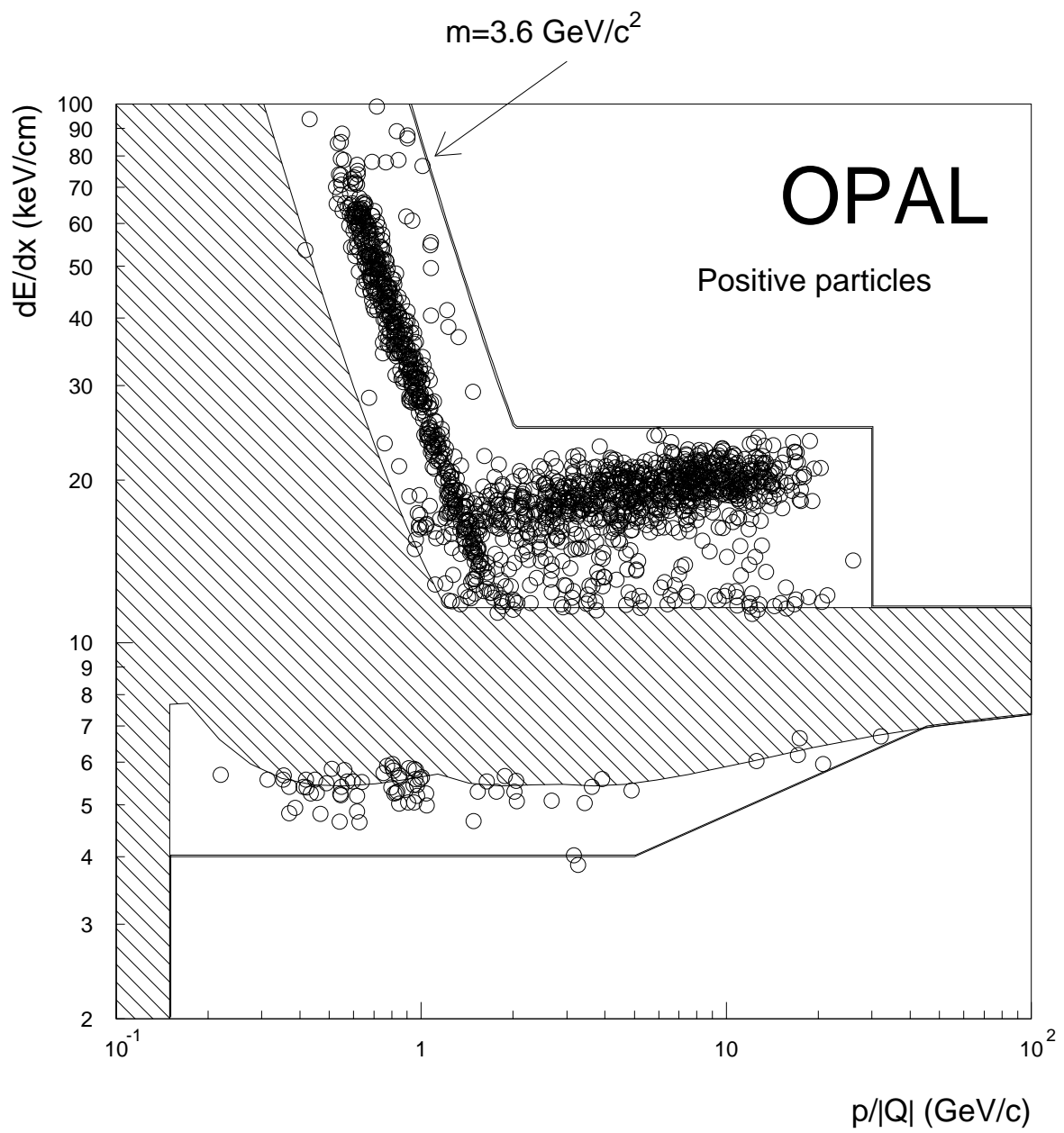


Fig. 2(a)

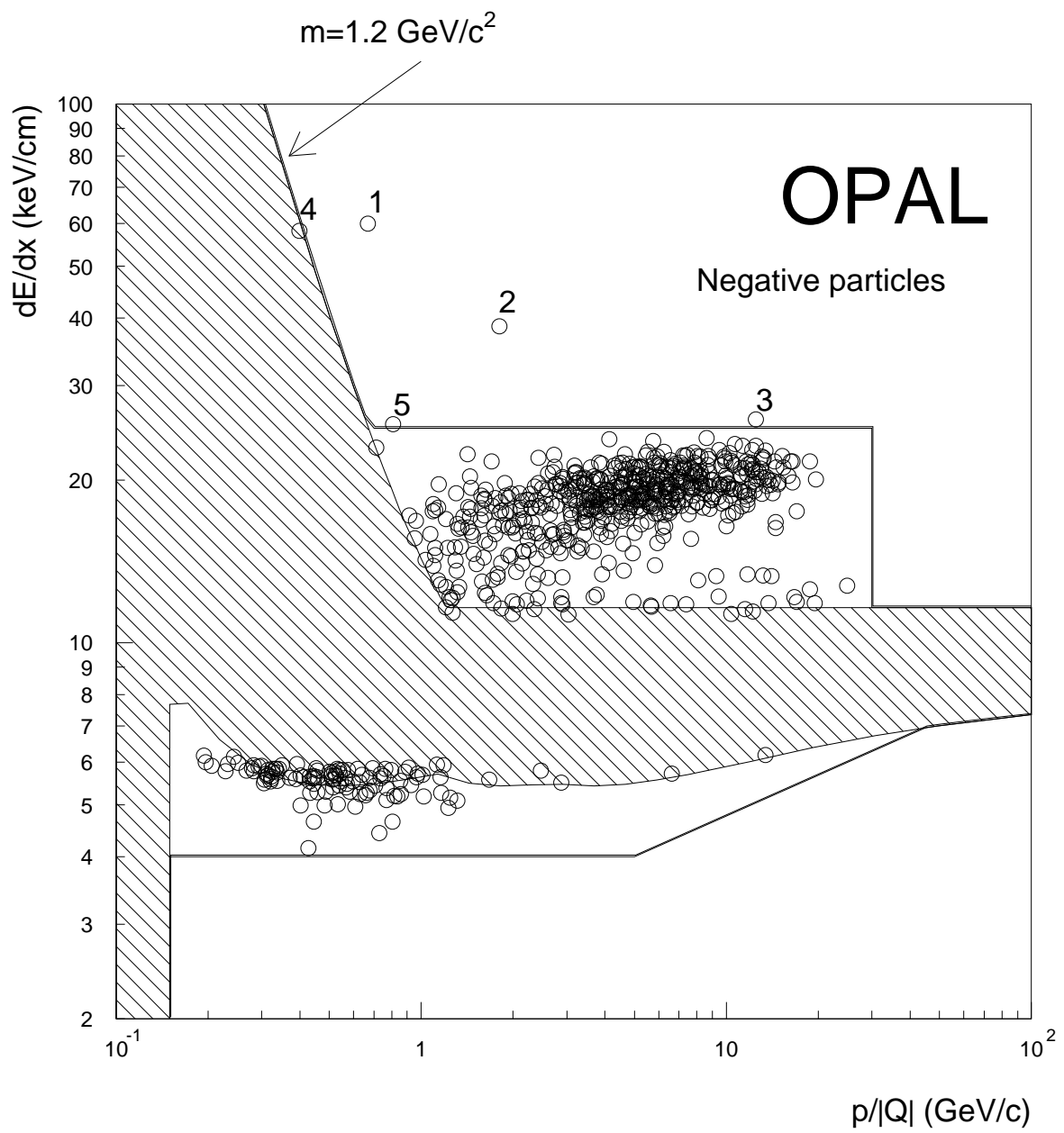


Fig. 2(b)

OPAL

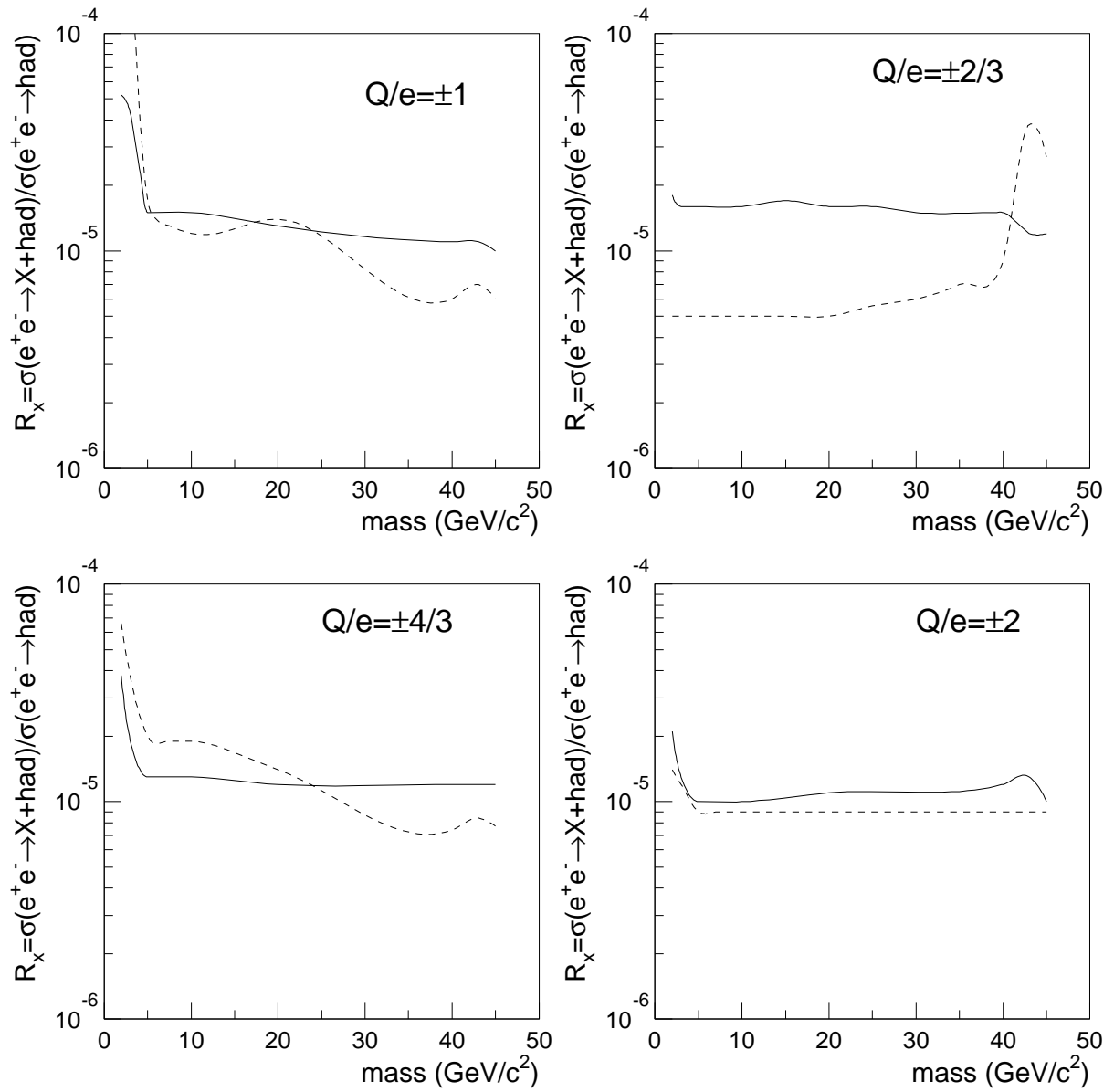


Fig. 3

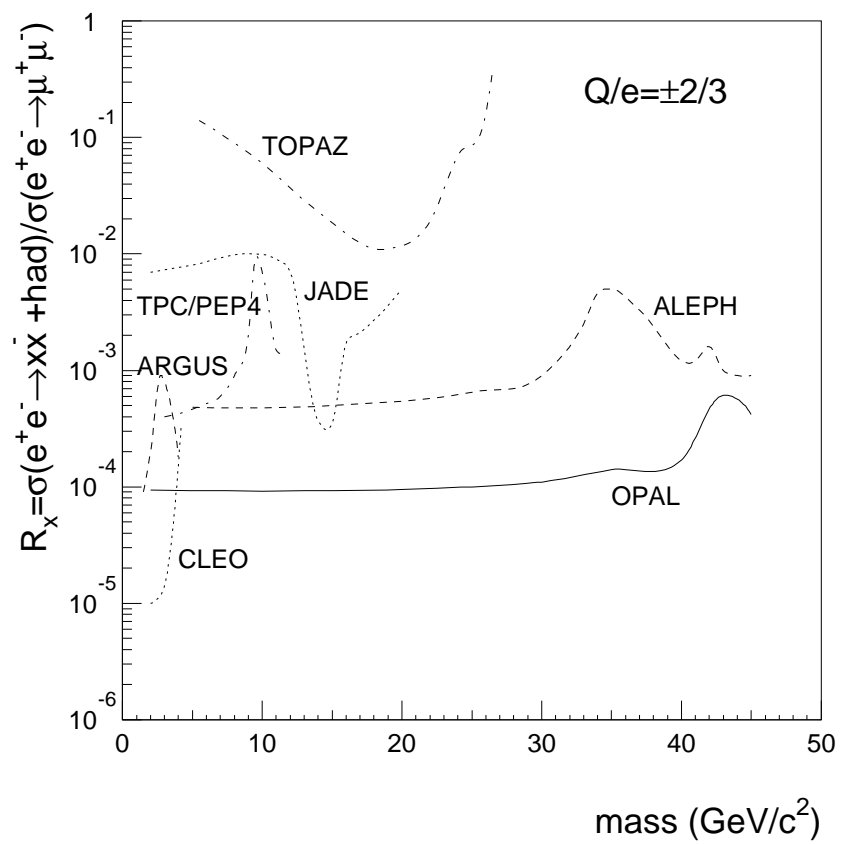


Fig. 4

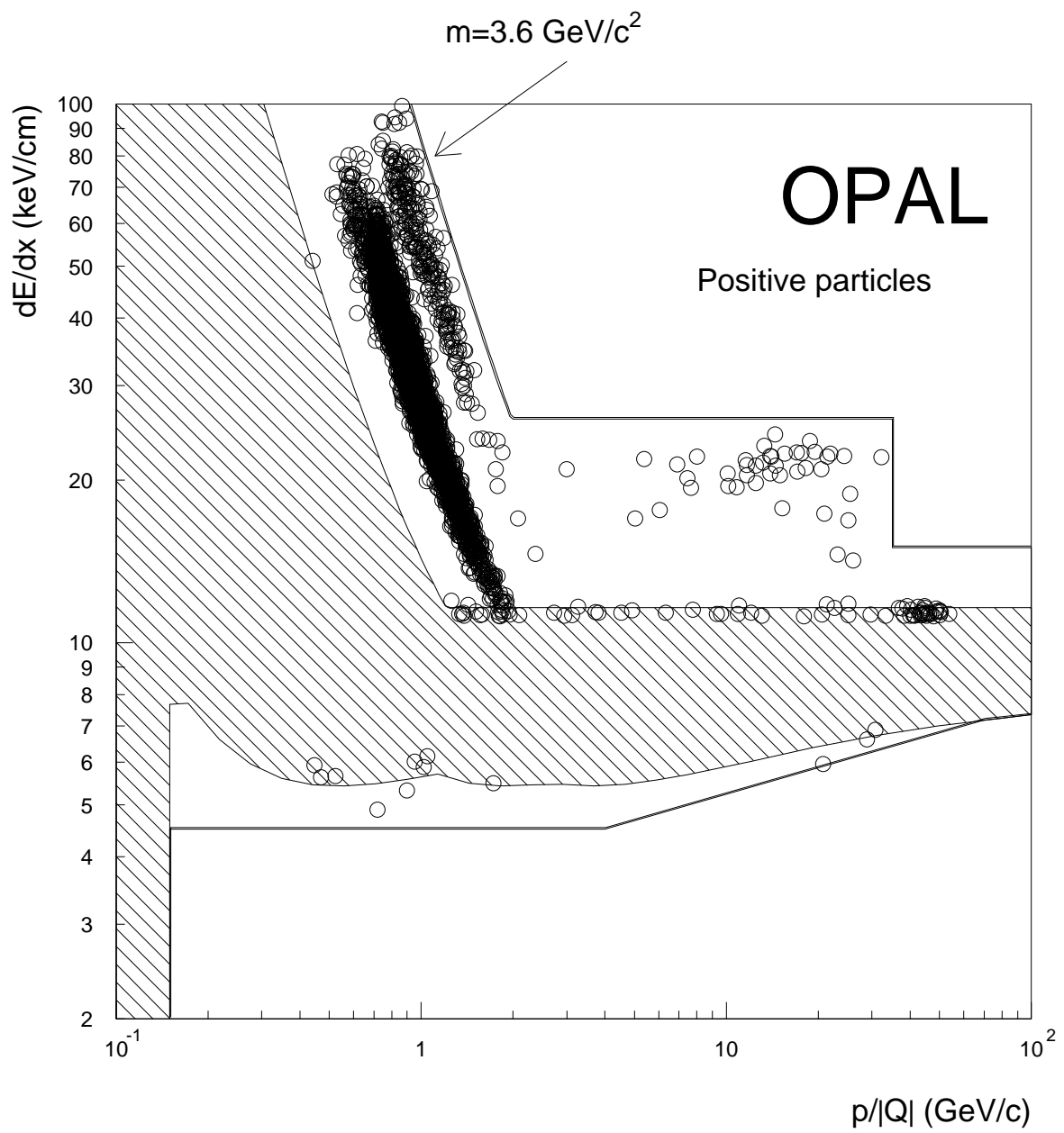


Fig. 5(a)

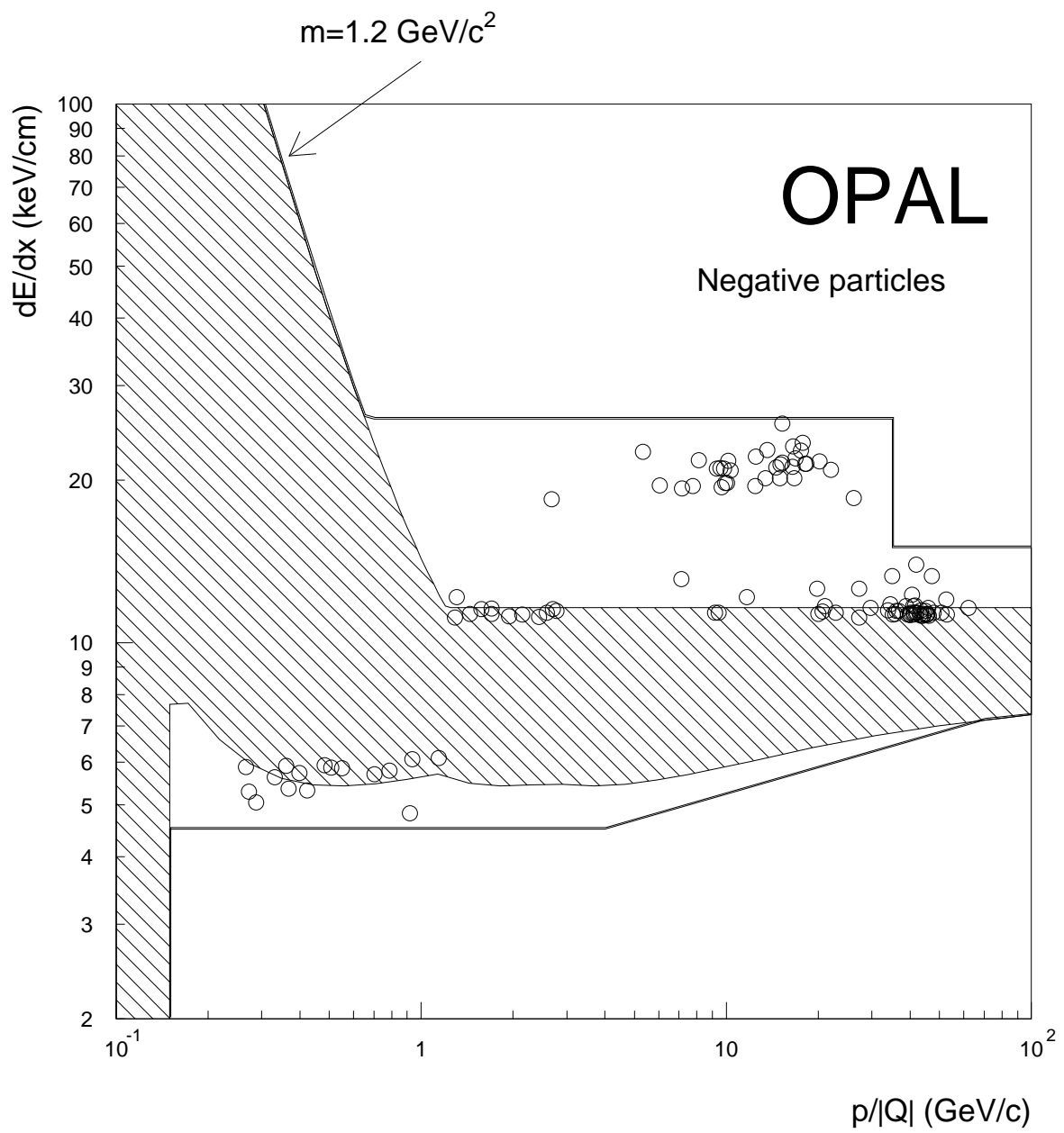


Fig. 5(b)